Available online at www.sciencedirect.com
SCIENCE DIRECT®
Journal of Molecular Catalysis A: Chemical 212 (2004) 359–364
JOURNAL OF MOLECULAR CATALYSIS A: CHEMICAL
www.elsevier.com/locate/molcata

NCO formation from CO and NH species over Rh_2 A density functional theory study

Ricardo M. Ferullo, Norberto J. Castellani*

Departamento de Física, Universidad Nacional del Sur, Av. Alem 1253, 8000 Bahía Blanca, Argentina

Received 1 September 2003; received in revised form 5 December 2003; accepted 8 December 2003

Abstract

In the present work, the density functional theory formalism was used to study the reaction between coadsorbed CO and NH species, the last coming from ammonia decomposition, to form NCO over Rh_2. The optimized structures for each stage of the reaction were obtained and a μ^2(N,C)–CONH precursor state towards the NCO formation was found. The transition states structures were also modeled, which allowed to analyze the reaction pathway. When CO and NH species approach each other, they form easily the precursor state. From this stage, it decomposes to NCO and H surpassing an activation barrier of 1.17 eV. This picture is in agreement with the infrared spectroscopy results obtained in the reaction of CO with NH_3 over Rh/Al_2O_3 catalysts: a gradual decreasing of the feature assigned to the precursor state with a parallel increasing of the characteristic band due to the NCO asymmetric stretching mode.

Keywords: Density functional theory; NCO formation; Rh catalyst

1. Introduction

In the past, it has been proposed that the catalytic reaction between CO and NH_3 plays a major role in the production of cyanamide, an intermediate to obtain dicyanamide, a very effective nitrification inhibitor [1,2]. The CO/NH_3 reaction could also be a step in the global process taking place in three way catalysts (TWC) where NO, CO and H_2 are important species [3]. In a series of earlier works, it was established that the isocyanate (NCO) surface group is a competitive species facing cyanamide [4–7]. Indeed, when the reaction takes place over a Rh/Al_2O_3 catalyst no surface reaction was observed at 100 K. But at temperatures greater than 230 K, the formation of isocyanate species was observed [7]. This surface species has been also detected on the surface of the metal phase of other supported catalytic systems [4–6]. Several proposals have been given about the mechanism of isocyanate formation in this reaction using Rh/SiO_2 and Ru/Al_2O_3 at low temperatures [4,6]. In one of them, the formation of an amide intermediate is involved.

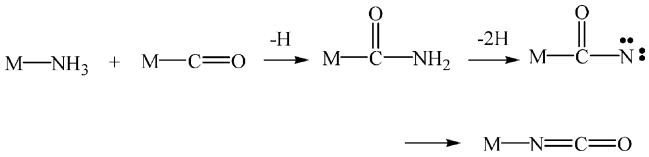

(1)

A second mechanism, for Ru/Al_2O_3 at high temperatures and for Pd/SiO_2 at low and high temperatures, considers the reaction of atomic N with CO [5,6].

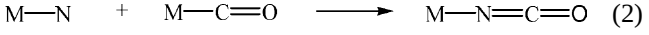

(2)

More recently, Paul and Marten proposed that a bridge-bound complex Rh–(OC ← NH) could be formed by nucleophilic attack of Rh–NH on the carbonyl C of Rh_x(CO) surface species [7], this mechanism being valid at least for low temperatures.

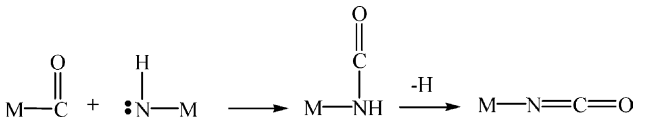

(3)

An increasing interest has been focussed on the behaviour of the isocyanate (NCO) surface group in other type of

* Corresponding author. Tel.: +54-2914595141; fax: +54-2914595142.
E-mail address: castella@criba.edu.ar (N.J. Castellani).

1381-1169/$ – see front matter © 2004 Elsevier B.V. All rights reserved.
doi:10.1016/j.molcata.2003.12.011

catalytic reactions that do not include H_2, particularly in the catalytic reduction of NO by CO. These reactions have been extensively studied in the last years due to their importance in automotive emission control. It has been well established that the NCO species is produced on active sites of supported transition metals catalysts like Pt/MgO, Rh/SiO_2, Cu–ZSM-5 and Rh/TiO_2 [8–11]. Infrared (IR) spectroscopy studies indicate that isocyanate migrates onto the support where it finally resides and accumulates. For this reason, it is believed that this surface compound behaves as an intermediate and does not participate in the NO reduction. However, very recently some experimental studies using IR and transient mass spectroscopy (MS) techniques performed over Rh/TiO_2 system suggest that NCO could act, at least under certain conditions, as an intermediate in the production of N_2O [11].

The goal of this work is to study theoretically the interaction between coadsorbed CO and NH species over rhodium using first principle methods. For this purpose, the role played by a Rh active site constituted by only two atoms was considered. In this way we attain, as it will be shown later, a reasonable qualitative picture of the interactions taken place on Rh catalysts.

2. Theoretical background

The calculations of this work have been performed within the density functional theory (DFT) using the Becke's three parameters hybrid nonlocal exchange functional combined with the Lee–Yang–Parr gradient-corrected correlation functional (B3LYP) [12] as implemented in the software package Gaussian 98 [13]. The basis set is all electron 6–31G** on H, C, N and O atoms. For Rh, an effective core potential including relativistic effects was used, with a [8s6p4d/3s3p2d] basis set for the $4s^2 4p^6 4d^8 5s^1$ valence electrons [13,14]. The quadratically convergent self-consistent field (SCF) technique based on the method of Bacskay [15] was applied. For the geometry optimization, the Berny algorithm [16] was used.

The model for the active site is a minimal cluster of two Rh atoms, allowing to study the interaction of two adsorbed species on the rhodium surface. This active site is supposed to be included in a surface relatively plane. Therefore, among all possible equilibrium geometries, the *cis* structures are only analyzed. Moreover, the different bonds are free to rotate or stretch on the same plane. Under this assumption, the optimization process simplifies largely. Hence, in the calculations the C–Rh–Rh–N dihedral angle was taken equal to zero degrees, while the rest of the parameters were fully optimized.

First principles calculations applying metal cluster models have been extensively employed in the past to study the adsorption and reaction properties of metallic surfaces. Particularly, the attention has been focussed to molecular or dissociative adsorption, coadsorption and surface diffusion. However, less interest was observed to study associative and/or interchange reactions between adsorbed species, like in the case of $CO + NH_3$ on supported Rh. Our interest is to give a theoretical approach to this last specific problem.

Clusters with 20–30 atoms are usually used to represent the interaction with infinite extended metal surfaces, although smaller clusters often describe reasonably the catalytic properties of highly dispersed supported metal particles. On the other hand, the active sites are normally related to irregularities of metal surfaces as kinks or steps, where atoms have low coordination numbers. These atoms could be assimilated to small naked clusters in an inert matrix or a naked atom or small clusters, susceptible to careful and accurate theoretical calculations. For example, Duarte and Salahub have reported [17] a study of the interaction between two molecules of NO over Ni_2 in order to describe the formation of the dimer $(NO)_2$. The presence of this dimer on several transition metal surfaces has been suggested by experimental results [18,19]. The scission of H–H bond when H_2 reacts with Pt_n or Pd_n ($n = 1$–3) has been studied by Nakatsuji et al. [20]. More recently, the effect of a second metal was considered in the H_2 + PtSn reaction [21]. Sometimes, caution has to be taken to study the adsorption of molecules like O_2 on small clusters as Ag_3 because exaggerated electron transfers are obtained when this molecule approaches the cluster [22]. This property is not observed for the isolated O atom for which, however, a correct description of the oxygen–silver interaction can be given. When the bonding of a molecule or molecular fragment to the metal cluster can be successfully predicted, molecular properties as the vibrational spectra can be reasonably described. For instance the C–O vibrational modes on Pd or Rh are well reproduced using Pd_2 [23] or a Rh atom [24] as metal substrate clusters, respectively. Noticeably, this approach of molecule–surface interaction resembles that adopted in organometallic compounds, which provide the first source of analysis for IR spectra of adsorbed molecules.

The atomic charges were calculated by using the natural bond orbital (NBO) population analysis [25]. On the other hand, the concept of overlap population (OP) from Mulliken population analysis [26] was applied to study the bond strength between two atoms.

3. Results and discussion

In order to study the Rh–CO + Rh–NH → Rh–NCO + Rh–H reaction different optimized structures were considered for each stage of the reaction: (a) the "initial state" with the CO and NH species linked to each Rh atom, (b) a possible "precursor state" towards the formation of NCO, and (c) the "final state" with the NCO group and the H atom separately bonded to the Rh atoms. These states will be denoted as IS, PS and FS, respectively. For each case, the multiplicity M of the complete molecular system was varied from 1 to 5 in order to obtain the minimal energy.

Table 1
Relative total energy with respect to the structure with lowest energy (in eV) for the initial (IS), precursor (PS) and final (FS) states

Multiplicity	IS	PS	FS
1	1.17	0.65	1.19
3	1.16	0.00	0.64
5	1.59	0.60	–

In Table 1, the total molecular energies are reported. They are expressed relatively to the structure with lowest energy. At the three stages, the minimal energy corresponds to $M = 3$ with an electronic $^3A''$ state, although at the IS the energies for $M = 1$ and $M = 3$ are nearly the same. It is important to note that, at the FS, the electronic state corresponding to $M = 5$ the *cis* geometry is not formed.

The optimized geometries, indicating their respective equilibrium distances and angles, are pictured in Fig. 1. For the IS and FS states, they are close to the situations where the species are constrained to lie on top over the metallic atoms, the C–Rh1–Rh2, H–Rh1–Rh2 and N–Rh2–Rh1 angles being exactly equal to 90°. The geometrical structures with minimal energy are only 0.17 and 0.13 eV more stable than the constrained ones for the IS and the FS states, respectively. The Rh–Rh distance decreases slightly during the reaction. The nucleophilic attack produces an intermediate that has the structure resembling that of the isocyanic acid, HNCO. The N–C bond of this adsorbed species is 0.1 Å longer than the same distance calculated for free HNCO. This bond is formed at the cost of an important increase of the Rh–C and Rh–N distances by 0.192 and 0.174 Å, respectively. On the other hand, the N–C and C–O distances for the FS are slightly greater than those calculated for free HNCO, which are 1.218 and 1.174 Å, respectively. It is interesting to underline that Solymosi and Kiss [27] proposed that the HNCO molecule interacts with Pt(1 1 0) surface also via the N and C atoms, i.e., giving a similar structure to that we found at the PS.

The atomic NBO charges are reported in Table 2. The first important observation is that the C and N atoms have

Table 2
NBO atomic charges for the initial (IS), precursor (PS) and final (FS) states

	IS	PS	FS
Rh1	−0.127	+0.226	+0.394
Rh2	+0.347	+0.216	+0.044
O	−0.450	−0.573	−0.514
C	+0.565	+0.573	+0.803
N	−0.642	−0.860	−0.740
H	+0.308	+0.418	+0.012

relevant positive and negative charges at all the stages of the reaction, making feasible an electrostatic interaction between the corresponding δ^+ and δ^- charge centers and giving the conditions to initiate a nucleophilic attack (C ← N). It is interesting to note that after the overall reaction takes place the C atom becomes more positively charged and the N atom more negatively charged, respectively. In order to understand this behavior, an analysis of different electron transfers within the molecular system was performed, based on data of Table 2. For this purpose, the atomic charge variations during each IS → PS and PS → FS chemical transition were computed. Moreover, these charge modifications are supposed to be due only to electron transfers between first atomic neighbors, neglecting other possible direct electronic interchanges between next near atomic neighbours. So, during IS → PS the adsorbed species receive an amount of 0.222*e* from the Rh dimer and during PS → FS, practically no electrons are transferred between them. However, an internal electron movement of 0.168*e* is produced from Rh1 to Rh2. The first IS → PS transition is accompanied by electron transfers of 0.123*e* from the C atom to the O atom and of 0.110*e* from the H atom to the N atom. During the PS → FS, transition there is a significant movement of 0.406*e* to the H atom. If the electronic charge of NCO as a group is considered, we obtain an electron charge decrease of 0.409*e*, practically the amount received by the H atom. This atom links at the FS with Rh1, which remains more positively charged due to the above commented Rh1 → Rh2 electron transfer. At the same FS state, the NCO group

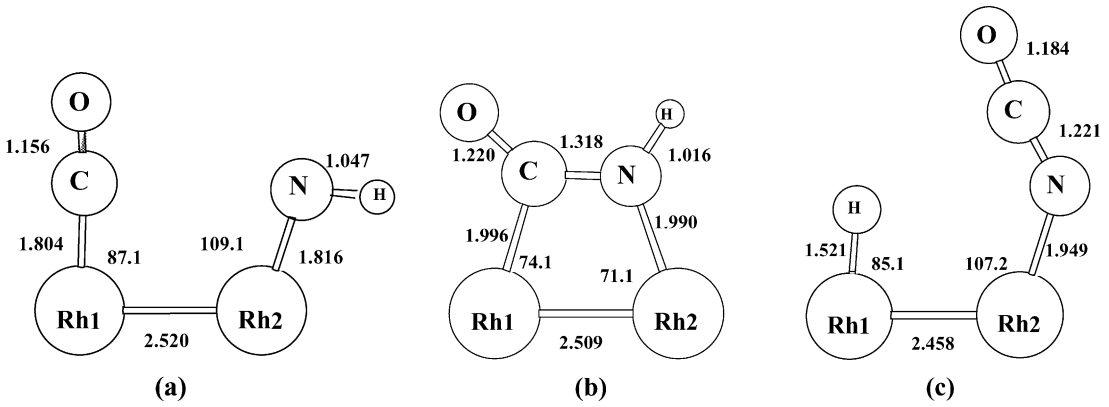

Fig. 1. Optimized structures for (a) initial state (IS); (b) precursor state (PS); and (c) final state (FS). Distances are in Å and angles in degrees.

Table 3
Infrared spectroscopy frequencies for the most intense lines (in cm^{-1})

IS		PS		FS	
539	ν(RhC)	691	ν(RhC) + ν(RhN)	428	ν(RhN)
670	ν(RhN)	1168	δ(NH)[a]	496	δ(RhH)[a]
798	δ(NH)[a]	1202	ν(NC)	1361	ν(NCO, sym.)
2083	ν(CO)	1807	ν(CO)	2196	ν(RhH)
3173	ν(NH)	3554	ν(NH)	2233	ν(NCO, asym.)
2076	Experimental[b]	1970	Experimental[c]	2170	Experimental[d]

[a] Bending in plane.
[b] Assigned to ν(CO) for CO bonded on top over Rh in Rh/Al_2O_3 catalysts [7].
[c] Assigned to a perturbed ν(CO) mode bridge-bonded by NH surface species in Rh/Al_2O_3 catalysts [7].
[d] Assigned to ν(NCO) asymmetric mode for NCO adsorption over Rh in Rh/Al_2O_3 catalysts [7].

becomes largely polarized, the C atom being the δ^+ charge center and N and O the δ^- charge centers.

Regarding the vibrational frequencies, the most intense features calculated at each stage are summarized in Table 3. The value corresponding for CO stretching at the IS is similar to that assigned to CO adsorption on top geometry for Rh/Al_2O_3 catalysts. The calculated asymmetric NCO stretching mode at FS is also in agreement with experimental observations over Rh containing catalysts [7]. In fact, Paul and Marten observed two intensive peaks at 2170 and 2246 cm^{-1} which were attributed to the NCO interaction with Rh and Al_2O_3, respectively. Besides, these features gradually grew with time exposure and temperature. At the same time, this growth was consistent with the gradual decreasing of a band at 1970 cm^{-1}. These authors assigned the last to a precursor complex, previous to NCO formation. It was suggested that, after NH_3 decomposition and production of NH species [28], this precursor complex is formed on Rh by the nucleophilic attack of NH onto the C atom of CO (OC ← NH). They proposed a precursor with a η^1(N)–CONH structure, i.e., linked to the metal via the N atom (see Eq. (3)). From this intermediate, the NCO group would be finally formed by eliminating the H atom. The frequency calculated at the PS (Table 4), which is due to the stretching mode of CO along its axis, could correspond to the above mentioned precursor state. However, our calculations predict a different structure, μ^2(N,C)–CONH, where both N and C atoms are linked to the metal dimer.

Table 4
Overlap populations for optimized structures and transition states

	IS	TS1	PS	TS2_I	TS2_II	FS
Rh–Rh	0.250	0.316	0.360	0.335	0.340	0.397
Rh–C	0.711	0.661	0.474	–	–	–
Rh–N	0.507	0.393	0.329	0.265	0.140	0.357
C–O	1.213	1.190	1.024	1.266	1.197	1.249
N–H	0.490	0.569	0.667	0.178	0.692	–
N–C	0.002	0.076	0.626	1.175	0.796	1.165

The decreasing of the CO stretching frequency can be explained by considering that the nucleophilic attack of NH produces an increasing of the $2\pi^*$ population of CO. Indeed, Mulliken analysis predicts a population of the π orbitals of 0.43*e* and 0.97*e* for IS and PS, respectively.

We mention that, to our knowledge, the only theoretical calculation carried out at the present about the interaction between isocyanate and Rh is due to Paul et al. [4]. These authors performed ab initio calculations using a model in which the NCO species interacts with a single Rh atom via the N atom. The linear configuration resulted to be the geometry with minimal energy, and the obtained N–C and C–O distance values were 1.175 and 1.201 Å, respectively. On the contrary, our calculations predict a N–C distance longer than the C–O one. On the other hand, the Rh–N bond length (1.917 Å) is close to that calculated here (1.949 Å). Concerning the NCO frequencies, Paul et al. obtained a value of 2419 cm^{-1}, which is around 190 cm^{-1} higher than our result (2233 cm^{-1}). In comparison, the experimental value is 2170 cm^{-1} for NCO adsorption on Rh/Al_2O_3 catalysts [7] and 2230 cm^{-1} for rhodium complexes [29].

The transition states (TS) between the IS and the PS, and between PS and the FS were also considered. We will denote them as TS1 and TS2, respectively. In the first case, the geometry pictured in Fig. 2(a) was the optimized one. For this structure, the adsorbed species approach each other, keeping at about 2 Å in between. The energy barrier corresponding to the IS → PS transition results to be relatively low (0.49 eV).

On the other hand, two different transition states labeled as TS2_I and TS2_II were found between PS and FS, depending on the geometry of the final state. In the first situation, pictured in Fig. 2(b), the N atom is linked to the same Rh2 atom both at the TS and the FS. This is precisely the case considered in Fig. 1. In order to reach this geometry, the H atom must rotate around the N–Rh axis. While the N–H bond is breaking, the H–Rh bond is forming. The corresponding activation barrier is 1.17 eV. In the other mechanism, the NH group is inserted between the C and O atoms, resulting a structure where only the N atom is bonded to the dimmer, as it pictured in Fig. 2(c). The NCO is finally linked with Rh1 atom. In this case the activation barrier is somewhat higher (1.27 eV).

The different bond strengths were analyzed using the overlap population (OP) definition, which values are summarized in Table 4. A slight increase of the OP of the Rh–Rh bond, OP(Rh1–Rh2), was observed during the reaction. The Rh–C and Rh–N links decrease their strength when the PS is reached together with the formation of the N–C bond. In the next step, the OP(Rh–N) becomes very high when the NCO is finally formed. The C–O bond strength decreases drastically at the PS, when compared with respect to the IS. Concerning the transition states, the non negligible OP(N–C) value at TS1 indicates an approaching between CO and NH species, and a significant weakening of OP(N–H) is clear at the TS2_I state, while its value is large at the TS2_II state

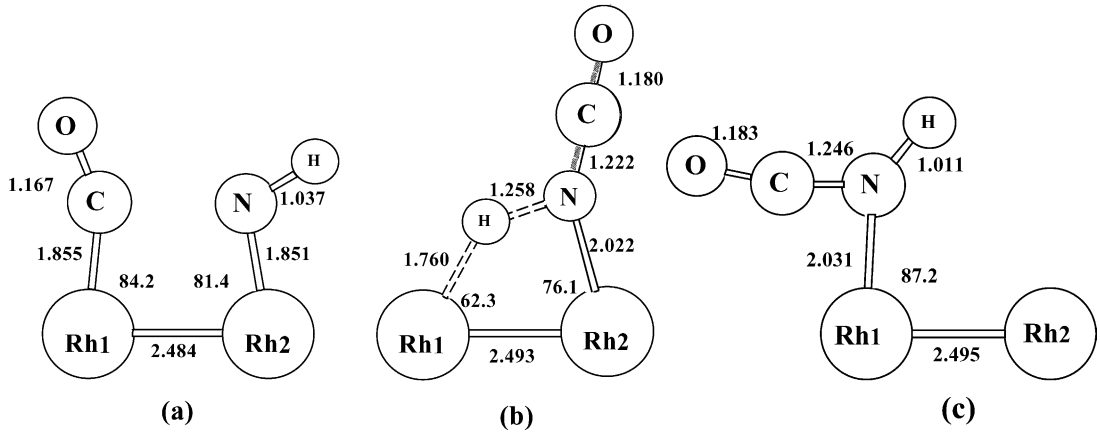

Fig. 2. Optimized structures for the transition states (see text): (a) TS1; (b) TS2_I; and (c) TS2_II. Distances are in Å and angles in degrees.

(even slightly greater than at the PS state). All this observations are in agreement with the changes in the interatomic distances discussed above.

The potential energy profile of the reaction is presented in Fig. 3. From this, a qualitative description of the reaction is possible to be made. When CO and NH species approach each other they form easily the precursor state surpassing an activation barrier of 0.49 eV. At this stage, the last species can return to the initial state, surpassing a barrier of 1.65 eV, or it can decompose to NCO and H, a more favourable situation from the energetic point of view. Another possibility that can be considered is to reach the TS2_1 through the TS2_2 rather than directly. Subsequently, from the FS the NCO species would evolve by diffusing on the metal surface and finally migrating to the support. It is also interesting to note that because our calculations predict a link with the metal via the N and C atoms at the PS, the model of reaction presented here have similarities with both mechanisms proposed in the past, i.e., Eqs. (1) and (3).

Finally, the validity of using the Rh_2 cluster was tested recomputing the three most stable structures using Rh_2 and Rh_4 clusters, both with the Rh–Rh distance fixed at the bulk value (2.69 Å). These calculations show that the general picture outlined previously for the energy profile is retained. For the fixed dimer, the energy differences between IS and PS, and between PS and FS increase slightly (in both cases by nearly 0.07 eV) with respect to the relaxed dimer. The optimized geometries obtained using a Rh_4 tetrahedron were performed constraining the calculation on a plane perpendicular to the [0 0 1] direction. Here, the minimal energies correspond to a higher multiplicity ($M = 7$). The energy difference between IS and PS results to be 1.70 eV, i.e., about 0.5 eV higher than the case of the relaxed dimer. In addition, the energy difference between PS and FS increases also nearly 0.5 eV. Therefore, for the two considered tests the relative stability of the three structures is the same than that calculated for the dimer where the Rh–Rh distance was allowed to relax.

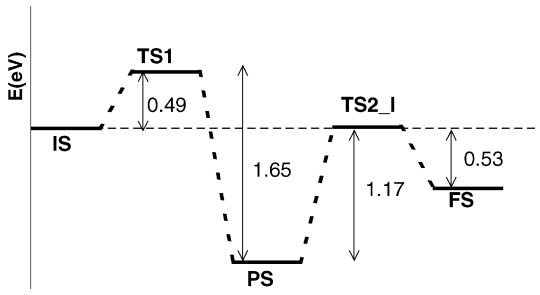

Fig. 3. Potential energy of the CO + NH reaction.

4. Conclusions

Using the density functional formalism and a simple cluster model the CO + NH reaction to yield NCO was qualitatively described. The reactive species form easily a μ^2(N,C)–CONH precursor state, which produce the isocyanate complex surpassing an activation barrier of 1.17 eV. This picture is in complete agreement with the results obtained in the reaction of CO with NH_3 over Rh/Al_2O_3 catalysts using infrared spectroscopy: a gradual decreasing of the feature assigned to a precursor state with a parallel increasing of the band due to NCO asymmetric stretching mode.

Acknowledgements

Financial support from CONICET and UNS are gratefully acknowledged.

References

[1] L.G. Boatright, J.S. Macay, US Patent 2,721,786 (1955).
[2] W.R. Rollingson, US Patent 2,975,032 (1961).
[3] D.C. Chambers, D.E. Angove, N.W. Cant, J. Catal. 204 (2001) 11.

[4] D.K. Paul, M.L. McKee, S.D. Worley, N.W. Hoffman, D.H. Ash, J. Gautney, J. Phys. Chem. 93 (1989) 4598.
[5] D.K. Paul, S.D. Worley, N.W. Hoffman, D.H. Ash, J. Gautney, J. Catal. 120 (1989) 272.
[6] D.K. Paul, S.D. Worley, N.W. Hoffman, D.H. Ash, J. Gautney, Surf. Sci. 223 (1989) 509.
[7] D.K. Paul, C.D. Marten, Langmuir 14 (1998) 3820.
[8] F. Solymosi, L. Völgyesi, J. Sárkány, J. Catal. 54 (1978) 336.
[9] W.C. Hecker, A.T. Bell, J. Catal. 85 (1984) 389.
[10] F. Solymosi, T. Bánsági, J. Catal. 156 (1995) 75.
[11] D. Kondarides, T. Chafik, X. Verykios, J. Catal. 193 (2000) 303.
[12] A.D. Becke, J. Chem. Phys. 98 (1993) 5648.
[13] Gaussian 98 (Revision A.7), M.J. Frisch, G.W. Trucks, H.B. Schlegel, G.E. Scuseria, M.A. Robb, J.R. Cheeseman, V.G. Zakrzewski, J.A. Montgomery, R.E. Stratmann, J.C. Burant, S. Dapprich, J.M. Millam, A.D. Daniels, K.N. Kudin, M.C. Strain, O. Farkas, J. Tomasi, V. Barone, M. Cossi, R. Cammi, B. Mennucci, C. Pomelli, C. Adamo, S. Clifford, J. Ochterski, G.A. Petersson, P.Y. Ayala, Q. Cui, K. Morokuma, D.K. Malick, A.D. Rabuck, K. Raghavachari, J.B. Foresman, J. Cioslowski, J.V. Ortiz, B.B. Stefanov, G. Liu, A. Liashenko, P. Piskorz, I. Komaromi, R. Gomperts, R.L. Martin, D.J. Fox, T. Kieth, M.A. Al-Laham, C.Y. Peng, A. Nanayakkara, C. Gonzalez, M. Challacombe, P.M.W. Gill, B.G. Johnson, W. Chen, M.W. Wong, J.L. Andres, M. Head-Gordon, E.S. Replogle and J.A. Pople, Gaussian, Inc., Pittsburgh PA, 1998.
[14] P.J. Hay, W.R. Wadt, J. Chem. Phys. 82 (1985) 299.
[15] G.B. Bacskay, Chem. Phys. 61 (1981) 385.
[16] H.B. Schlegel, in: D.R. Yarkony (Ed.), Modern Electronic Structure Theory, World Scientific, Singapore, 1995.
[17] H.A. Duarte, D.R. Salahub, J. Phys. Chem. B 101 (1997) 7464.
[18] T.U. Bartke, R. Franchy, H. Ibach, Surf. Sci. 272 (1992) 299.
[19] A. Ludviksson, C. Huang, H.J. Jänsch, R.M. Martin, Surf. Sci. 284 (1993) 328.
[20] H. Nakatsuji, Y. Matsuzaki, T. Tonezawa, J. Chem. Phys. 88 (1988) 5759.
[21] S. Castillo, E. Poulain, V. Bertin, A. Cruz, Int. J. Quantum Chem.: Quantum Chem. Symp. 29 (1995) 207.
[22] E.A. Carter, W.A. Goddard III, Surf. Sci. 209 (1989) 243.
[23] P.S. Bagus, G. Pacchioni, Surf. Sci. 236 (1990) 233.
[24] M.L. McKee, S.D. Worley, J. Phys. Chem. 92 (1988) 3699.
[25] A.E. Reed, L.A. Curtiss, F. Weinhold, Chem. Rev. 88 (1988) 899.
[26] I.N. Levine, Quantum Chemistry, fifth ed., Prentice-Hall, New Jersey, 2000, p. 505.
[27] F. Solymosi, J. Kiss, Surf. Sci. 108 (1981) 641.
[28] A. Vavere, R.S. Hansen, J. Catal. 69 (1981) 158.
[29] W.C. Hecker, A.T. Bell, J. Catal. 85 (1984) 389.